

Sintering behavior and characteristic of bio-based hydroxyapatite coating deposited on titanium

M. A. Roudan^a, S. Ramesh^{a,*}, Y.H. Wong^a, H. Chandran^b, S. Krishnasamy^c, W.D. Teng^d and L.T. Bang^e

^aCentre of Advanced Manufacturing and Materials Processing, Department of Mechanical Engineering, Faculty of Engineering, University of Malaya, 50603 Kuala Lumpur, Malaysia

^bDivision of Neurosurgery, Faculty of Medicine, University of Malaya, 50603 Kuala Lumpur, Malaysia

^cDepartment of Surgery, Faculty of Medicine, University of Malaya, 50603 Kuala Lumpur, Malaysia

^dCeramics Technology Group, SIRIM Berhad, 40911 Shah Alam, Malaysia

^eDepartment of Biomaterials, Faculty of Dental Science, Kyushu University, Fukuoka, Japan

Deposition of hydroxyapatite derived from bio-waste eggshell on titanium substrate via electrophoretic deposition method and the thermal stability of the resulting coating were investigated. The coated substrates were sintered at different temperatures ranging from 900 °C to 1100 °C in argon atmosphere prior to characterisation. The results indicated that a crack-free HA coating layer having an average thickness of 20 µm was successfully deposited at the optimum temperature of 1050 °C. The XRD analysis indicated that the sintered coated substrates were fully HA phase and were stable up to 1050 °C, with Ca/P ratio of 1.67. The SEM results showed that good bonding was achieved between the HA coating and the Ti substrate. There was also no secondary phase formation at the joint interface. This study demonstrates the viability of using electrophoretic deposition method to coat a thin layer of bio-based HA onto titanium without disrupting the biocompatibility nature of the HA phase.

Key words: Hydroxyapatite, Eggshells, Electrophoretic deposition, HA coating; Sintering.

Introduction

Hydroxyapatite (HA) is one of the widely researched materials because of its diverse applications especially in biomedical engineering. The biocompatibility nature and the chemical structure of this material being similar to that of hard tissues enables HA to integrate well with natural bone. One of the major limitations of HA is the low mechanical properties such as hardness and fracture toughness ($\leq 1 \text{ MPam}^{1/2}$) which restrict its usage to low-load bearing applications [1-5]. Hence, much work is still required to improve the mechanical properties of HA. Such initiatives have focussed on improving the synthesis method and the sintering of hydroxyapatite using conventional as well as non-conventional techniques.

The preparation of HA mostly focussed on using the hydrothermal, mechanochemical, sol-gel and wet chemical methods. Different starting precursors were used and subjected to a variety of process steps. Nevertheless, in all cases, calcium and phosphate are normally the main composition found in the precursors. For example, the source of phosphate could be from phosphoric acid and

the calcium source would be calcium oxide or calcium carbonated. Calcium oxide can be derived from natural sources such as eggshell, seashell, bovine and chicken bones. Depending on the starting precursors and the method of synthesis, different quality of final product could be produced, particularly resulting in a stoichiometric or nonstoichiometric HA characterised by having different powder morphology and particle size.

One of the ways to expand the usage of HA for load-bearing applications would be to coat HA on metallic implant such as titanium and stainless steel. This is another way to achieve the combination of substrate strength and biocompatibility of coated surface which makes the implant viable for load bearing devices [6-10]. For instance, Blind et al. [11] reported that HA coating allows for quick osteo-integration to take place between the metallic implant surface and bony tissues. According to the literatures, the hydroxyapatite coating could also serve to improve the corrosion resistance of the metallic implant [12-13].

Many coating techniques have been investigated such as plasma spraying, thermal spraying, sputter coating, electrophoretic deposition and dip coating. Surface quality and thickness of deposited film would depend on the coating process. All of these techniques have their advantages and disadvantages. In particular, electrophoretic deposition is one of the favourable methods used for hydroxyapatite coating. Simple setup

*Corresponding author:
Tel : +603 7967 5209
Fax: +603 7967 7621
E-mail: ramesh79@um.edu.my

and the ability to apply the coating on complex shape at a desired thickness of coating layer are the main advantages of this process [14-15].

In terms of sintering, there are many consolidation methods that can be employed to densify hydroxyapatite which include the conventional method, hot isostatic pressing and microwave sintering. The conventional sintering is the most widely used technique although this method requires very slow heating rate and can be time consuming if compared to microwave sintering which takes minutes to sinter the ceramic [16-21].

The objective of present study was to evaluate the feasibility of using electrophoretic deposition method to coat a thin layer of bio-based hydroxyapatite derived from eggshells on titanium substrate. The HA phase stability and morphological evolution of the coated layer when sintered at temperatures ranging from 900 °C to 1100 °C were examined.

Experimental procedures

In this study, hydroxyapatite synthesized from eggshell through a wet chemical method [22] was used as coating material. The derived HA powder was subsequently calcined using an electrical box furnace at 900 °C for 1 hr, while heating and cooling rate was kept constant at 10 °C per min. In order to achieve a homogenous particles, the calcined powder was milled together with ethanol as liquid medium, using a planetary ball mill for 4 hrs at 100 rpm. The slurry was dried at 60 °C for 24 hrs. For the preparation of the coating suspension, 0.05 g of calcined hydroxyapatite powder was added to 20 ml ethanol and sonicated for 20 min. A drop of 1 M hydrochloric acid was added to the suspension as dispersing agent to control the motion of particles in the colloid.

Commercially available pure titanium (Ti) sheet was used as substrate in this study. The sheet was cut to small pieces as the substrate (2 mm thickness × 10 mm width × 20 mm length). The substrate surface was prepared by grinding using a SiC paper of fine abrasive grade P1000. The substrates were then cleaned ultrasonically for 10 min. prior to deposition.

For the electrophoretic deposition, the electrodes, Ti substrate and stainless steel, were washed with distilled water, then submerged in acetone and sonicated for 15 min. prior to coating. The dried substrates were attached to an electrical crocodile clips, faced to each other with 1 cm distance between them, and connected to electrophoretic power supplier (EPS601-GE Healthcare-USA). For the purpose of coating, a current of 400 mA, power of 100 W and 25 V voltage were applied on the substrates for 6 min. Upon the completion of deposition process, coated substrates were dried at room temperature and subjected to cold isostatic pressing at 200 MPa. The coated substrates were then sintered at different temperatures ranging from 900 °C to 1100 °C, at a heating rate of 5 °C/min., under flowing argon gas in a

tube furnace. The sintered substrates was cut vertically using a linear precision saw (Isomet 5000-Buehler-USA) at speed of 3000 rpm and feeding rate of 0.5 mm per minute for cross section examination.

The morphology of the synthesized eggshell-derived hydroxyapatite particles was performed using a transmission electron microscope (TEM, Carl Zeiss, Libra-Germany). For this purpose, the hydroxyapatite powder was mixed in ethanol and sonicated for 1 hr followed by two days aging. A small amount of suspension was applied on a copper grid and dried at room temperature for two days prior to analysis. Thermal stability of hydroxyapatite from room temperature to 1000 °C with 5 °C/min. heating rate was investigated using a TGA/DTA analyser (Perkin Elmer Pyris Diamond TG/DTA).

Phase analysis by X-ray diffraction (XRD: Empyrean, PANalytical, The Netherlands) of the powder and coated substrates were carried out under ambient conditions using Cu-K α as the radiation source operating at 45 kV in step mode with a 0.02 ° 2 θ step and a count time of 0.5 sec per step over the 2 θ range 20 ° to 60 °. The diffraction peaks of XRD patterns were studied by using the Xpert-High Score Plus software.

Microstructure characterization, cross sectional view of the coating interface and elemental analysis of coated substrates were carried out by using scanning electron microscope (SEM), coupled with Energy Dispersive X-ray spectroscopy (EDS) analyzer (Hitachi TM3030, Japan).

Results and Discussion

The morphology of the eggshell-derived HA particles are shown in Fig. 1. The starting HA exhibited a needle-like nanostructured particles, with an average

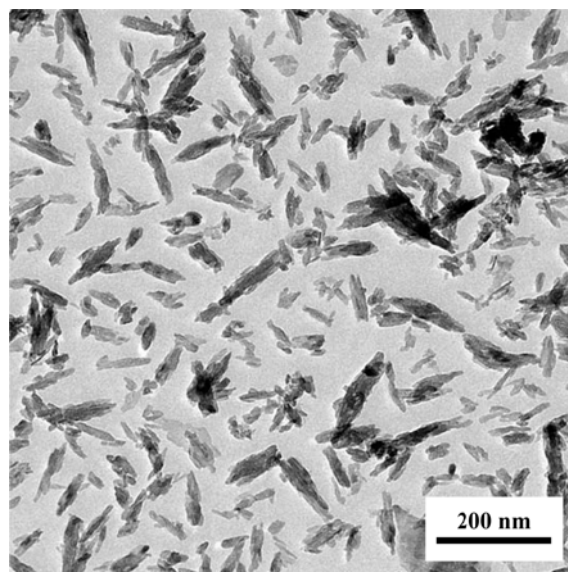


Fig. 1. TEM image of eggshell-derived HA powder.

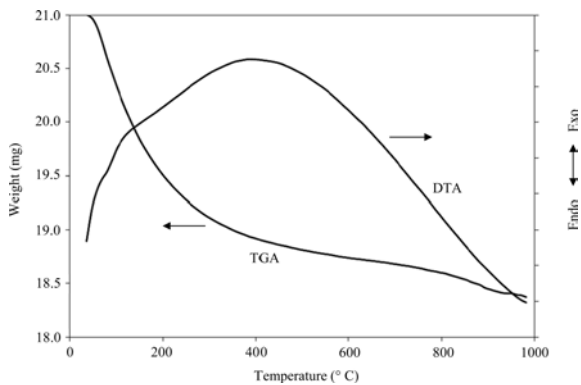


Fig. 2. TGA/DTA analysis of eggshell-derived HA powder.

size length of 50 ± 10 nm. This morphology is typical for wet-chemical precipitated HA and could vary depending on the powder processing method employed to synthesis the HA [23-28]. The morphology of the particle has an effect on the mobility of the charged particles and could influence the coating process [29]. Nevertheless, the needle-like particles has been reported to exhibit better sinterability when compared to other particle morphologies [30].

The DTA/TGA curve of synthesized hydroxyapatite is shown in Fig. 2. A broad exothermic band starting from 90 °C and centered at about 400 °C was observed and this could be attributed to the crystallization of hydroxyapatite. This phenomenon was also accompanied by a sharp weight loss of about 10% at 400 °C and increased further to 12% at 1000 °C, believed to be associated with the loss of dehydrated water in the HA lattice [30-33].

Visual observation of the sintered coated substrates indicated that sintering at 1100 °C was detrimental as it resulted in the delamination of the HA coating. Hence, subsequent analysis was focused on substrates sintered up to 1050 °C. The XRD signatures of sintered substrates at 900 to 1050 °C are shown in Fig. 3. The XRD analysis revealed the formation of pure and highly crystalline HA as confirmed by comparing to the standard JCPDS reference card number 00-009-0432 for hydroxyapatite. There was no secondary phase formation such as tricalcium phosphate or tetracalcium phosphate. The intensity of all peaks including the highest peak at $2\theta = 31.78^\circ$ corresponding to (211) lattice plane, increased with increasing sintering temperatures. The changing of the broad peaks to sharp peaks at higher temperatures is related to phase transition from amorphous to crystalline which is believed to start at 400 °C based on the DTA analysis. Based on the XRD analysis, sintering at 1050 °C has been identified as the optimum sintering temperature as the coating composed of highly crystalline HA phase which is favourable for biomedical application. In general, the synthesized HA derived from eggshell in the present work exhibited good thermal stability when

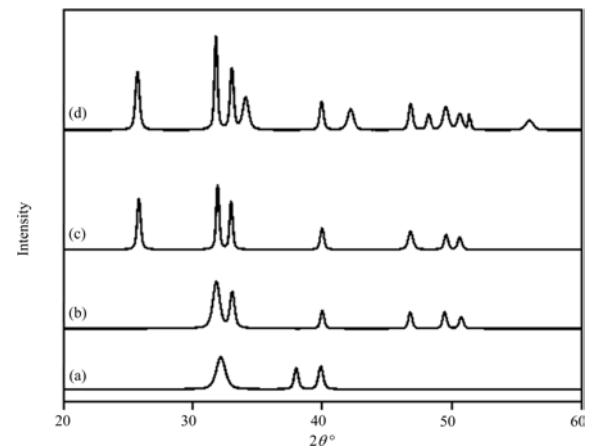


Fig. 3. XRD patterns of coated substrates sintered at various temperatures: (a) 900 °C, (b) 950 °C, (c) 1000 °C and (d) 1050 °C. All peaks corresponded to the HA phase.

sintered up to 1050 °C when compared to that reported by other researchers who noted the decomposition of hydroxyapatite proceeded at about 930 °C [15, 34-36].

The SEM microstructure of the HA coating sintered at various temperatures is shown in Fig. 4. As can be observed that the deposition was successful as there is no visible crack or pinhole in the coating, as typically shown in Fig. 4(e) for HA coating sintered at 1050 °C. In addition, regardless of sintering temperatures, a homogeneous HA structure, comprising of an equiaxed grain morphology having a uniform size across the surface can be noted from Figs. 4(a-d) thus demonstrating that the starting HA powder and the deposition conditions employed in the present work were feasible. The results also indicated that a uniform and relatively dense layer of HA, particularly for substrates sintered at 1000 °C and 1050 °C were deposited on titanium. Sintering above 1050 °C is not favorable as delamination of the HA layer was observed. This phenomenon could be associated with the oxidization of the substrate at high temperatures and could result in the degradation of HA phase [37-39].

The EDX analysis of sintered HA coating at 1050 °C is presented at Fig. 5. A similar profile was noted for other sintering temperatures. The presence of elements such as Mg, Si and K were expected as it is associated to the eggshell which is used as the starting calcium precursor. The existence of these elements in the HA coating is favourable since such elements are generally found in natural bone composition [27, 33]. Calcium and phosphate are the major peaks detected by EDS analysis, and according to the data, the Ca/P ratio of the HA coating was calculated to be about 1.67. This value differs from the values of 1.5 to 1.65 as reported by several authors and can be attributed to the different processing method employed and precursors used to synthesis the HA powder [40, 41].

A typical cross-sectional view of the coated substrate sintered at 1050 °C is presented in Fig. 6. A relatively

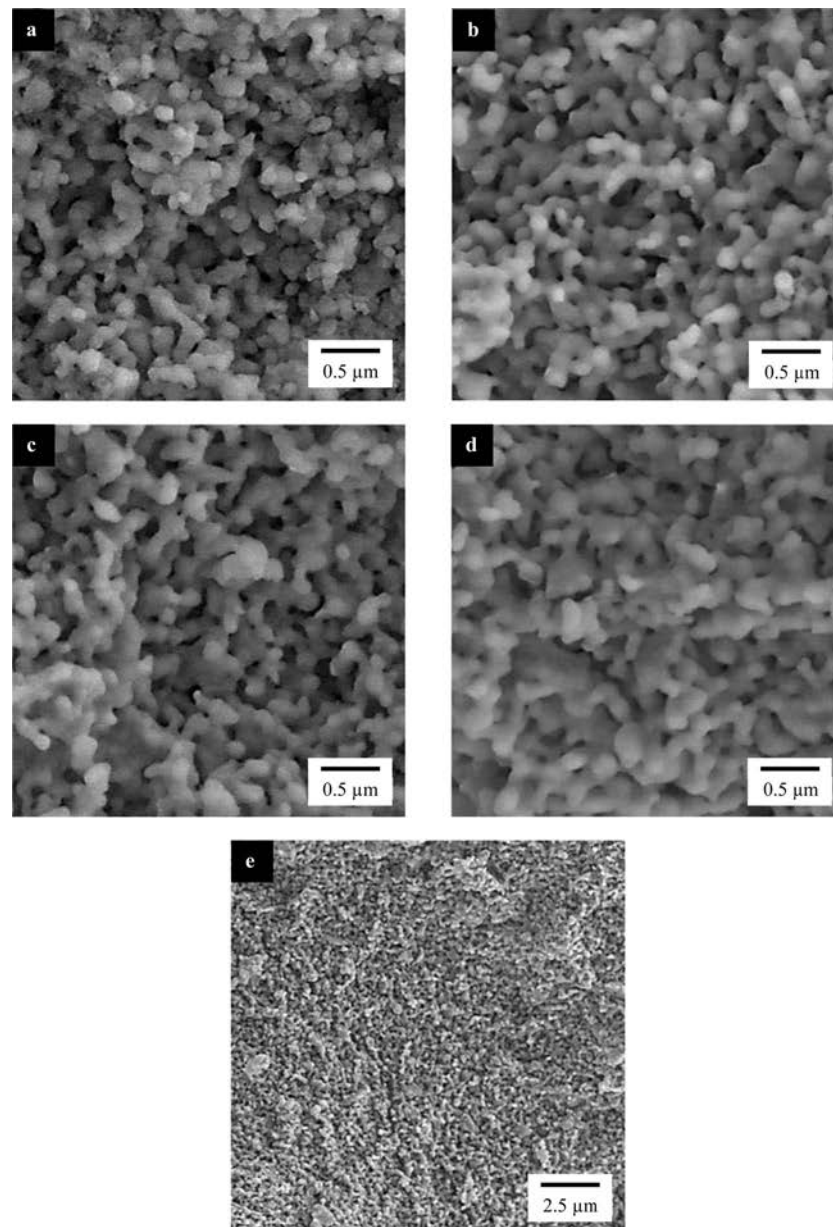


Fig. 4. SEM images of HA coating sintered at (a) 900 °C, (b) 950 °C, (c) 1000 °C and (d & e) 1050 °C.

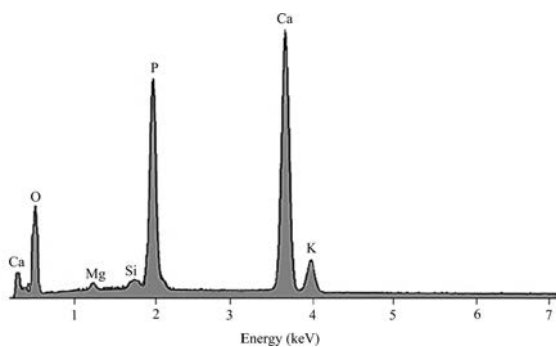


Fig. 5. Typical EDX analysis of sintered HA coating at 1050 °C.

uniform layer with an average thickness of about 20 μm was formed by deposition process. As can be seen in the SEM image, the coating and substrate

exhibited excellent bonding with each other. This result indicated that the good adhesion between the HA layer and the substrate obtained by electrophoretic deposition could be related to the nano-sized particles of the HA powder, believed to have played a role in reducing the thermal expansion mismatch between the HA and substrate during sintering [37, 42-45].

The cross sectional view and the compositional profile of the coated substrate sintered at 1050 °C are shown in Fig. 7. It can be observed that a good bonding exist at the interface of the substrate and HA layer. The compositional signatures of Ca, P and Ti as measured along the x - y - z line and superimposed on the SEM micrograph in Fig. 7 indicated that there was no reaction between the Ti and HA. A smooth transition in the compositional profile can be observe at the bonding

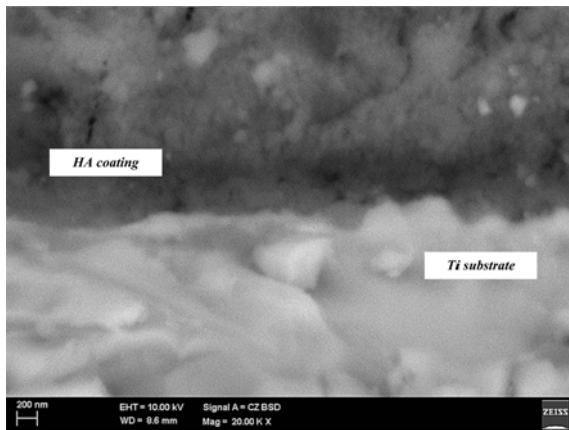


Fig. 6. SEM images of the cross-sectional area of HA coated substrate sintered at 1050 °C.

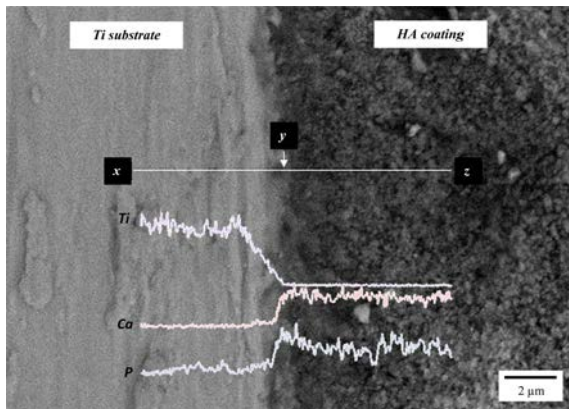


Fig. 7. SEM image of HA coated substrate sintered at 1050 °C showing the nature of the bonding at the interface between the HA coating/Ti substrate and compositional analysis across the interface.

interface “point y” as shown in Fig. 7. This results show that the electrophoretic deposition employed in the present work was successful in depositing HA onto Ti substrate without inducing any secondary phase formation.

Conclusions

The process of coating eggshell-derived hydroxyapatite synthesized via a wet chemical precipitation on titanium substrate through electrophoretic deposition method and the sintering behaviour of the deposited HA layer was investigated. The results indicated that a crack-free and phase pure crystalline hydroxyapatite was deposited successfully on the Ti substrate. The HA phase was not disrupted and was stable up to 1050 °C, however delamination of the coating occurred when sintered at 1100 °C. Based on the SEM and phase composition analysis, sintering at 1050 °C was found to be the optimum condition to produce a highly crystalline HA coating characterised by having a homogeneous structure, comprising of equiaxed grain morphology. This study has demonstrated the viability of employing eggshell as

the starting calcium precursor to produce needle-like HA particles suitable for use as coating for titanium based on electrophoretic deposition method.

Acknowledgments

This study was supported under the PPP Grant No. PG078-2015A.

References

- O. Prokopiev and I. Sevostianov, *Mater. Sci. & Eng. A431*[1] (2006) 218-227.
- A. Clifford, M.S. Ata and I. Zhitomirsky, *Mater. Letts.* 201 (2017) 140-143.
- W. Pon-On, P. Suntornsaratoon, N. Charoenphandhu, J. Thongbunchoo, N. Krishnamra and I.M. Tang, *Mater. Sci. & Eng. C 62* (2016) 183-189.
- H. Liu, H. Peng, Y. Wu, C. Zhang, Y. Cai, G. Xu and H.W. Ou Yang, *Biomater.* 34[18] (2013) 4404-4417.
- S. Ramesh, C.J. Gan, L.T. Bang, A. Niakan, C.Y. Tan, J. Purbolaksono and W.D. Teng, *J. Ceram. Proc. Res.* 16[6] (2015) 683-689.
- M. Sadat-Shojai, M.T. Khorasani, E. Dinpanah-Khoshdargi and A. Jamshidi, *Acta Biomaterialia*, 9[8] (2013) 7591-7621.
- M.N. Hassan, M.M. Mahmoud, A.A. El-Fattah and S. Kandil, *Ceram. Int.* 42[3] (2016) 3725-3744.
- A. Kazemi, M. Abdellahi, A. Khajeh-Sharafabadi, A. Khandan and N. Ozada, *Mater. Sci. & Eng. C71* (2017) 604-610.
- S. Ramesh, A.N. Natasha, C.Y. Tan, L.T. Bang, C.Y. Ching and H. Chandran, *Ceram. Int.* 42[6] (2016) 7824-7829.
- M.P. Ferraz, F.J. Monteiro and C.M. Manuel, *J. Appl. Biomater. & Biomech.* 2[2] (2004) 74-80.
- O. Blind, L.H. Klein, B. Dailey and L. Jordan, *Dental Mater.* 21[11] (2005) 1017-1024.
- A. Stoch, A. Brożek, G. Kmita, J. Stoch, W. Jastrzebski and A. Rakowska, *J. Molecular Struc.* 596[1] (2001) 191-200.
- C.T. Kwok, P.K. Wong, F.T. Cheng and H.C. Man, *Appl. Surf. Sci.* 255[13] (2009) 6736-6744.
- A.R. Boccaccini, S. Keim, R. Ma, Y. Li and I. Zhitomirsky, *J. Royal Soc. Interface*, 7[Suppl 5] (2010) S581-S613.
- I. Zhitomirsky and L. Gal-Or, *J. Mater. Sci.: Mater. Med.* 8[4] (1997) 213-219.
- S. Ramesh, C.Y. Tan, S.B. Bhaduri, W.D. Teng and I. Sopyan, *J. Mater. Proc. Tech.* 206[1] (2008) 221-230.
- S. Nath, B. Basu and A. Sinha, *Trends in Biomater. & Artificial Organs.* 19[2] (2006) 93-98.
- Z. Yang, Y. Jiang, Y. Wang, L. Ma and F. Li, *Mater. Letts.* 58[27] (2004) 3586-3590.
- S. Panyata, S. Eitssayeam, G. Rujijjanagul, T. Tunkasiri and K. Pengpat, *Adv. Mater. Res.* 506 (2012) 190-193.
- S. Pramanik, A.K. Agarwal, K.N. Rai and A. Garg, *Ceram. Int.* 33[3] (2007) 419-426.
- A. Niakan, S. Ramesh, C.Y. Tan, A. Shukor, M. Hamdi and W.D. Teng, *Appl. Mech. & Mater.* 372 (2013) 177-180.
- M.A. Roudan, S. Ramesh, A. Niakan, Y.H. Wong, M.A. Zavareh, Hari Chandran and U. Sutharsini, *J. Ceram. Proc. Res.* 18[1] (2017) 69-72.
- A. Pal, S. Paul, A.R. Choudhury, V.K. Balla, M. Das and A. Sinha, *Mater. Letts.* 203 (2017) 89-92.
- Z. Evis and T.J. Webster, *Adv. Appl. Ceram.* 110[5] (2011)

- 311-321.
25. N. Sahiner, C. Silan, S. Sagbas, P. Ilgin, S. Butun, H. Erdugan and R.S. Ayyala, *Microporous & Mesoporous Mater.* 155 (2012) 124-130.
 26. W.K. Chew, A. Niakan, N.A. Nawawi, L.T. Bang and S. Ramesh, *Inter. J. Automotive & Mech. Eng.* 12 (2015) 3089.
 27. M. Akram, R. Ahmed, I. Shakir, W.A.W. Ibrahim and R. Hussain, *J. Mater. Sci.* 49[4] (2014) 1461-1475.
 28. S. Ramesh, R. Tolouei, C.Y. Tan, K.L. Aw, W.H. Yeo, I. Sopyan and W.D. Teng, *Adv. Mater. Res.* 264 (2011) 1856-1861.
 29. B. Ferrari, A.J. Sanchez-Herencia and R. Moreno, *Mater. Letts.* 35[5] (1998) 370-374.
 30. S. Ramesh, A.N. Natasha, C.Y. Tan, L.T. Bang, A. Niakan, J. Purbolaksono and W.D. Teng, *Ceram. Int.* 41[9] (2015) 10434-10441.
 31. G.A. Martínez-Castañón, J.P. Loyola-Rodríguez, N.V. Zavala-Alonso, S.E. Hernández-Martínez, N. Niño-Martínez, G. Ortega-Zarzosa and F. Ruiz, *Superficies y vacío*, 25[2] (2012) 101-105.
 32. K. Prabakaran and S. Rajeswari, *Spectrochimica Acta Part A: Molecular & Biomolecular Spectroscopy* 74[5] (2009) 1127-1134.
 33. A. Niakan, S. Ramesh, P. Ganesan, C.Y. Tan, J. Purbolaksono, H. Chandran and W.D. Teng, *Ceram. Int.* 41[2] (2015) 3024-3029.
 34. S. Ramesh, C.Y. Tan, R. Tolouei, M. Amiriyan, J. Purbolaksono, I. Sopyan and W.D. Teng, *Mater. & Design* 34 (2012) 148-154.
 35. A. Rapacz-Kmita, C. Paluszkiwicz, A. Ślósarczyk and Z. Paszkiewicz, *J. Molecular Structure* 744 (2005) 653-656.
 36. P. Kamalanathan, S. Ramesh, L.T. Bang, A. Niakan, C.Y. Tan, J. Purbolaksono and W.D. Teng, *Ceram. Int.* 40[10] (2014) 16349-16359.
 37. M. Wei, A.J. Ruys, B.K. Milthorpe, C.C. Sorrell and J.H. Evans, *J. Sol-Gel Sci. & Tech.* 21[1] (2001) 39-48.
 38. M. Wei, A.J. Ruys, M.V. Swain, B.K. Milthorpe and C.C. Sorrell, *J. Mater. Sci.: Mater. Med.* 16[2] (2005) 101-106.
 39. A.J. Ruys, M. Wei, C.C. Sorrell, M.R. Dickson, A. Brandwood and B.K. Milthorpe, *Biomater.* 16[5] (1995) 409-415.
 40. S. Raynaud, E. Champion, D. Bernache-Assollant and P. Thomas, *Biomater.* 23[4] (2002) 1065-1072.
 41. M. Manso, C. Jimenez, C. Morant, P. Herrero and J.M. Martinez-Duart, *Biomater.* 21[17] (2000) 1755-1761.
 42. U.W. Jung, J.W. Hwang, D.Y. Choi, K.S. Hu, M.K. Kwon, S.H. Choi and H.J. Kim, *J. Periodontal & Implant Sci.* 42[2] (2012) 59-63.
 43. N. Eliaz, S. Shmueli, I. Shur, D. Benayahu, D. Aronov and G. Rosenman, *Acta Biomaterialia*, 5[8] (2009) 3178-3191.
 44. H. Gleiter, *Nanostructured Mater.* 1[1] (1992) 1-19.
 45. A.T. Rad, M. Solati-Hashjin, N.A.A.A. Osman and S. Faghihi, *Ceram. Int.* 40[8] (2014) 12681-12691.